New Phytologist

Research

Strigolactone biosynthesis is evolutionarily conserved, regulated by phosphate starvation and contributes to resistance against phytopathogenic fungi in a moss, *Physcomitrella patens*

Eva L. Decker[1], Adrian Alder[2], Stefan Hunn[1], Jenny Ferguson[1], Mikko T. Lehtonen[3], Bjoern Scheler[1], Klaus L. Kerres[1], Gertrud Wiedemann[1], Vajiheh Safavi-Rizi[2], Steffen Nordzieke[4], Aparna Balakrishna[5], Lina Baz[5], Javier Avalos[4], Jari P. T. Valkonen[3], Ralf Reski[1,6,7] and Salim Al-Babili[2,5]

[1]Plant Biotechnology, Faculty of Biology, University of Freiburg, Schaenzlestr. 1, Freiburg 79104, Germany; [2]Cell Biology, Faculty of Biology, University of Freiburg, Schaenzlestr. 1, Freiburg 79104, Germany; [3]Department of Agricultural Sciences, University of Helsinki, Latokartanonkaari 7, Helsinki FIN-00014, Finland; [4]Departamento de Genética, Facultad de Biología, Universidad de Sevilla, Seville E-41080, Spain; [5]BESE Division, Plant Science Program, King Abdullah University of Science and Technology (KAUST), Thuwal 23955-6900, Saudi Arabia; [6]FRIAS – Freiburg Institute for Advanced Studies, University of Freiburg, Freiburg 79104, Germany; [7]BIOSS – Centre for Biological Signalling Studies, University of Freiburg, Freiburg 79104, Germany

Authors for correspondence:
Salim Al-Babili
Tel: +966 12 8082565
Email: salim.babili@kaust.edu.sa

Ralf Reski
Tel: +49 761 203 6969
Email: ralf.reski@biologie.uni-freiburg.de

Received: *13 January 2017*
Accepted: *31 January 2017*

New Phytologist (2017) **216:** 455–468
doi: 10.1111/nph.14506

Key words: carlactone, carotenoid cleavage dioxygenase, carotenoids, *Orobanche ramosa*, phosphate starvation, *Physcomitrella patens*, *Sclerotinia sclerotiorum*, strigolactones.

Summary

- In seed plants, strigolactones (SLs) regulate architecture and induce mycorrhizal symbiosis in response to environmental cues. SLs are formed by combined activity of the carotenoid cleavage dioxygenases (CCDs) 7 and 8 from 9-*cis*-β-carotene, leading to carlactone that is converted by cytochromes P450 (clade 711; MAX1 in *Arabidopsis*) into various SLs. As *Physcomitrella patens* possesses *CCD7* and *CCD8* homologs but lacks *MAX1*, we investigated if PpCCD7 together with PpCCD8 form carlactone and how deletion of these enzymes influences growth and interactions with the environment.
- We investigated the enzymatic activity of PpCCD7 and PpCCD8 *in vitro*, identified the formed products by high performance liquid chromatography (HPLC) and LC-MS, and generated and analysed *ΔCCD7* and *ΔCCD8* mutants.
- We defined enzymatic activity of PpCCD7 as a stereospecific 9-*cis*-CCD and PpCCD8 as a carlactone synthase. *ΔCCD7* and *ΔCCD8* lines showed enhanced caulonema growth, which was revertible by adding the SL analogue GR24 or carlactone. Wild-type (WT) exudates induced seed germination in *Orobanche ramosa*. This activity was increased upon phosphate starvation and abolished in exudates of both mutants. Furthermore, both mutants showed increased susceptibility to phytopathogenic fungi.
- Our study reveals the deep evolutionary conservation of SL biosynthesis, SL function, and its regulation by biotic and abiotic cues.

Introduction

Strigolactones (SLs) are carotenoid-derived secondary metabolites originally isolated from root exudates due to their capability of inducing seed germination in root-parasitic weeds, such as *Striga* and *Orobanche* species (Cook *et al.*, 1966; for a review, see Xie *et al.*, 2010). Thus, the release of SLs into the soil initiates the attack by these parasites, which develop, following germination, a haustorium that connects them to the host roots and enables the uptake of water, minerals and sugars (Xie *et al.*, 2010; Ruyter-Spira *et al.*, 2013). However, the presence of SLs in root exudates also paves the way for establishing the beneficial symbiosis with mycorrhizal fungi, which may explain why plants are releasing these compounds (Akiyama *et al.*, 2005). SLs induce hyphal branching and promote the pre-symbiotic growth in these fungi, which is required to create the fungi–plant contact before establishing the mutualistic symbiosis in which plants get access to water, phosphorus and other minerals and, in return, supply the fungus with photosynthetic products (Akiyama *et al.*, 2005; Besserer *et al.*, 2008; Gutjahr & Parniske, 2013). Accordingly, plants release higher amounts of strigolactones upon phosphate starvation (Yoneyama *et al.*, 2012).

The discovery of several high-branching/-tillering pea, *Arabidopsis* and rice mutants has led to the identification of SLs as a 'new' plant hormone that determines the number of shoot branches and tillers by inhibiting the outgrowth of axillary buds in an auxin-dependent manner (Gomez-Roldan *et al.*, 2008; Umehara *et al.*, 2008). It was shown that *Arabidopsis more axillary branching* 1-4 (*Max*), several rice *high-tillering/dwarf* (*HTD*) and *dwarf* mutants (*d*), and *Ramosous* 1-5 (*rms*) are

affected either in the biosynthesis or in the perception of SLs, and that the high-branching phenotype of biosynthetic mutants can be – in contrast to perception mutants – rescued by external application of the SL analogue GR24 (Gomez-Roldan *et al.*, 2008; Umehara *et al.*, 2008). Subsequently, several developmental functions have been attributed to SLs, including induction of secondary growth, determining root architecture by inhibiting the growth of primary roots, and triggering the growth of lateral roots and root hairs. In addition, SLs accelerate senescence and are involved in the response of plants to abiotic stress (Brewer *et al.*, 2013; Kapulnik & Koltai, 2014; Seto & Yamaguchi, 2014; Waldie *et al.*, 2014; Al-Babili & Bouwmeester, 2015).

Strigolactones are derivatives of carotenoids, which are divided into the oxygen-free carotenes, such as β-carotene, and the xanthophylls that contain oxygen, such as lutein (Fraser & Bramley, 2004; Moise *et al.*, 2014; Nisar *et al.*, 2015). In addition, carotenoids differ in the *cis*/*trans*-isomeric state of their double bonds. Besides all-*trans*-configured carotenoids, plants synthesize and accumulate different *cis*-configured carotenoids that act as intermediates of the pathway, as light-harvesting pigments, or as precursors of phytohormones, for example abscisic acid (ABA) and SLs (Walter & Strack, 2011; Moise *et al.*, 2014; Al-Babili & Bouwmeester, 2015). The synthesis of ABA (Schwartz *et al.*, 1997) and other carotenoid-derived signalling molecules, such as the vertebrate retinoic acid (von Lintig, 2012), the fungal trisporic acid (Medina *et al.*, 2011) and SLs (Alder *et al.*, 2012), is initiated by oxidative cleavage of a double bond in the conjugated backbone of carotenoids, which is generally catalysed by carotenoid cleavage oxygenases (Giuliano *et al.*, 2003; Bouvier *et al.*, 2005; Moise *et al.*, 2005; Auldridge *et al.*, 2006; Walter & Strack, 2011).

The discovery that SLs deficiency is responsible for the more branching phenotype in different *Arabidopsis*, rice and pea mutants unravelled the involvement of four enzymes in SL biosynthesis (Seto & Yamaguchi, 2014; Al-Babili & Bouwmeester, 2015): the iron containing protein DWARF27 (Lin *et al.*, 2009); the carotenoid cleavage dioxygenases 7 (CCD7; Booker *et al.*, 2004; Zou *et al.*, 2006; Drummond *et al.*, 2009) and 8 (CCD8; Morris *et al.*, 2001; Sorefan *et al.*, 2003; Arite *et al.*, 2007; Simons *et al.*, 2007); and a cytochrome P450 clade 711 (MAX1 in *Arabidopsis*; Booker *et al.*, 2005). It was shown that DWARF27 catalyses the all-*trans*/9-*cis* reversible isomerization of β-carotene (Alder *et al.*, 2012; Bruno & Al-Babili, 2016). In the second step, CCD7 cleaves 9-*cis*-β-carotene into the volatile compound β-ionone and 9-*cis*-β-apo-10′-carotenal (Alder *et al.*, 2012; Bruno *et al.*, 2014). The latter is converted by CCD8 via a yet unelucidated combination of reactions into carlactone that resembles canonical SLs in the number of C atoms and the presence of a butenolide ring, which is connected to a second moiety via an enol ether bridge (Alder *et al.*, 2012). CCD8 enzymes also convert the all-*trans*-isomer of β-apo-10′-carotenal *in vitro*. However, in this case, they form a different product, the ketone all-*trans*-β-apo-13-carotenone (Alder *et al.*, 2008, 2012). The *Arabidopsis* MAX1 enzyme converts carlactone into carlactonoic acid that binds, after methylation, to the SL receptor α/β-hydrolase D14 (Abe *et al.*, 2014). However, methylcarlactonoic acid is not the final product of the *Arabidopsis* SL biosynthesis and is hydroxylated by the lateral branching oxidoreductase (LBO) into a yet unidentified compound (Brewer *et al.*, 2016).The α/β-hydrolase D14 mediates SL signalling by interaction with the F-box protein MAX2 that targets proteins to proteasomal degradation (Hamiaux *et al.*, 2012). In rice, carlactone is converted into the SL 4-deoxyorobanchol (*ent*-2′-*epi*-5-deoxystrigol) by the MAX1 homologue carlactone oxidase (Zhang *et al.*, 2014; Al-Babili & Bouwmeester, 2015). A further rice MAX1 homologue, orobanchol synthase, catalyses the formation of orobanchol, which is a widely distributed SL (Zhang *et al.*, 2014; Al-Babili & Bouwmeester, 2015).

The moss *Physcomitrella patens* is an excellent model organism to study the evolution of land plants in general (Menand *et al.*, 2007; Langdale, 2008; Rensing *et al.*, 2008; Prigge & Bezanilla, 2010; Weng & Chapple, 2010; Nelson & Werck-Reichhart, 2011) and the proposed role of phytohormones including SLs for the conquest of land by plants in particular (Bierfreund *et al.*, 2004; Vandenbussche *et al.*, 2007; Ludwig-Müller *et al.*, 2009; Paponov *et al.*, 2009; Stumpe *et al.*, 2010; Delaux *et al.*, 2012; Bennett *et al.*, 2014; Viaene *et al.*, 2014; Beike *et al.*, 2015; Lavy *et al.*, 2016). Despite the absence of a MAX1 homologue, previous studies on a *Physcomitrella Δ CCD8* mutant demonstrated that SLs are already present in this basal land plant (Proust *et al.*, 2011) and that these hormones are likely perceived by PpKAI2L proteins which are related to the D14 proteins of seed plants (Lopez-Obando *et al.*, 2016). *Physcomitrella* SLs were supposed to act as a quorum-sensing like signal regulating the growth of neighbouring colonies (Proust *et al.*, 2011), and to determine the plant morphology by regulating protonema branching, caulonemal cell elongation and cell division rates (Hoffmann *et al.*, 2014). However, it remained unclear, whether SLs/SL-like substances secreted by nonvascular plants such as *P. patens* have a role in interactions with other species.

In the present study, we investigated early steps in strigolactone biosynthesis in *P. patens* by characterizing the activity of the corresponding CCD7 and CCD8 enzymes, as well as the generation and analysis of *Δ CCD7* and *Δ CCD8* knockout mutants. Our data identify PpCCD7 as a stereospecific 9-*cis*-CCD and PpCCD8 as a carlactone synthase, and demonstrate that the path from β-carotene to carlactone is highly conserved in land plants. *Δ CCD7* and *Δ CCD8* moss mutants showed similar phenotypes, and an *Orobanche* seed germination assay revealed that in *P. patens* the release of SLs/related compounds is upregulated by phosphate starvation, indicating an evolutionarily conserved role of these compounds in shaping plant architecture in accordance to nutrient availability. Testing the susceptibility of the knockout mutants towards *Sclerotinia sclerotiorum* revealed a new function of SLs in supporting plant defence against phytopathogenic fungi.

Materials and Methods

Plasmid construction

All primers used for plasmid construction are listed in Supporting Information Table S1. To generate the *Physcomitrella patens*

carotenoid cleavage dioxygenase 7 (*PpCCD7*) knockout construct, genomic DNA fragments corresponding to the *pPCCD7* gene were amplified by PCR using the primers PpCCD7-KO1-FP_BamHI and PpCCD7-KO1-RP_BamHI that include *Bam*HI restriction sites. The obtained fragment was digested by *Bam*HI and ligated into accordingly digested and dephosphorylated pGEX-5X-3 (GE Healthcare), yielding the plasmid pGEX-5X-3-PpCCD7-KO1. The *nptII* resistance gene was then excised from pRT101neo (Girke *et al.*, 1998) by *Hin*dIII and ligated into *Hin*dIII-digested and dephosphorylated pGEX-5X-3-PpCCD7-KO1. The transformation fragment (2874 bp) containing the *nptII* resistance gene flanked by 880 bp 5′- and 494 bp 3′-*PpCCD7* genomic sequence was then obtained by digesting the resulting plasmid pGEX-5X-3-PpCCD7-KO1-nptII with *Apa*LI. The *Physcomitrella patens carotenoid cleavage dioxygenase 8* (*PpCCD8*) genomic fragment was amplified using the primers PHY-CCD8-G1 and PHY-CCD8-G2, and cloned into the pCR-Blunt, yielding the plasmid pCR-BLUNT-PpCCD8-KO1. The *hpt* sequence derives from plasmid pGAP-Hyg (Bitrián *et al.*, 2011) and had been PCR-amplified introducing *Hin*dIII sites to both ends and subsequently cloned to pJet1.2, resulting in pJet-hpt. Digestion of pJet-hpt by *Hin*dIII released the hpt-cassette that was then treated by T4-DNA polymerase and ligated into *Bsg*I digested and T4-DNA polymerase-treated pCR-BLUNT-PpCCD8-KO1, leading to pCR-BLUNT-PpCCD8-KO1-hpt. Digestion of the latter plasmid with *Sph*I/*Bam*HI yielded a 3233-bp fragment containing the *hpt* resistance gene flanked by 862 bp 5′- and 715 bp 3′-*PpCCD8* genomic sequence, which was used for transformation.

For investigating the enzymatic activity, *PpCCD7* cDNA was amplified from total cDNA, using the primers PhyCCD7 RP2 and Phy-CCD7 VII, and cloned into pCR-Blunt, yielding the plasmid pCR-BLUNT-PpCCD7as. For generation of the expression plasmid pTHIO-DAN1-PpCCD7dTP, *PpCCD7*dTP was amplified from pCR-BLUNT-PpCCD7as using the primers PhyCCD7dTP-ThioFP and PhyCCD7dTP-ThioRP, which contained *Xho*I and *Hin*dIII restriction sites, respectively. The truncated fragment lacking the transit peptide (144 bp from the start codon) was digested with *Xho*I/*Hin*dIII and ligated into accordingly digested pTHIO-DAN1 (Trautmann *et al.*, 2013), a derivative of pBAD/Thio-TOPO (Invitrogen). *PpCCD8* cDNA was amplified from total cDNA, using the primers PHY-CCD8 I and PHY-CCD8 II, and cloned into pCR-Blunt, yielding the plasmid pCR-BLUNT-PpCCD8. The expression plasmid pTHIO-DAN3-PpCCD8 was generated by digesting pCR-BLUNT-PpCCD8 with *Kpn*I/*Xba*I and ligating the isolated cDNA into accordingly treated pTHIO-DAN3, a derivative of pBAD/Thio-TOPO (Invitrogen).

Protein expression and isolation of enzyme preparations

pTHIO plasmids (pTHIO-DAN1-PpCCD7dTP, pTHIO-DAN3-PpCCD8, pTHIO-PsCCD7 (Alder *et al.*, 2012), pThio-Ps8 (Alder *et al.*, 2008), and the corresponding void plasmids) were transferred into BL21(DE3) *E. coli* cells harbouring the plasmid pGro7 (Takara Bio Inc.; Mobitec, Göttingen, Germany), which encodes the groES–groEL chaperone system under the control of an arabinose-inducible promoter. Cells were grown and harvested, and soluble fractions were isolated according to Alder *et al.* (2008) and used for *in vitro* assays.

Enzymatic assays

Substrates were prepared according to Ruch *et al.* (2005). Synthetic apocarotenals were kindly provided by BASF (Ludwigshafen, Germany). β-carotene and lycopene were obtained from Roth (Karlsruhe, Germany). 9-*cis*-β-carotene, 13-*cis*-β-carotene and 15-*cis*-β-carotene were obtained from Carotenature (Lupsingen, Switzerland). Zeaxanthin was isolated from *Synechocystis* sp. PCC6803, neoxanthin and lutein from spinach. β-apo-10′-carotenol and -carotenoic acid, produced by a NAD-dependent dehydrogenase from *Neurospora crassa* (Estrada *et al.*, 2008), were prepared according to Alder *et al.* (2008). Iodine-catalysed *cis*/*trans* isomerisation was performed according to Haugen *et al.* (1992) with some modifications: Carotenoids were dissolved in 50 ml n-hexan or dichlormethan and mixed with catalytic amounts of iodine (*c.* 2% of the carotenoid amount, dissolved in n-hexan). The solution was exposed to dim sunlight for 1 h, and carotenoids were then extracted using acetone and petroleum benzene/diethylether (1 : 4, v/v). *cis*/*trans* isomers were separated and collected by high performance liquid chromatography (HPLC) (see HPLC analyses).

Standard *in vitro* assays Standard *in vitro* assays were performed according to Alder *et al.* (2008) in a total volume of 200 µl containing 50 ml of soluble fraction of the corresponding overexpressing *E. coli* cells.

CCD7/CCD8 double assays CCD7/CCD8 double assays were performed according to Alder *et al.* (2008) in a total volume of 200 µl containing 40 µl of the soluble fraction of each enzyme.

HPLC analyses HPLC analyses were performed using a Waters separation system 2695 equipped with a photodiode array 12 detector (model 2996) and a YMC-Pack C30-reversed phase column (150 × 4.6 mm i.d., 5 µm; 22 YMC Europe, Schermbeck, Germany). Analysis was performed according to Bruno *et al.* (2014). For preparative separation of xanthophyll *cis*/*trans* isomers, we used the solvent systems B: MeOH/H2O/TBME (60 : 12 : 12, v/v/v) and A: MeOH/TBME (50 : 50, v/v). The column (YMC-Pack C30-reversed phase column, 150 × 4.6 mm i.d., 5 µm; 22 YMC Europe) was developed at a flow rate of 2.4 ml min^{-1} of 50% solvent system A, followed by a gradient to 80% A within 20 min and finally to 100% A within 2 min. The column was then washed for 6 min with 100% A at a flow rate of 3 ml min^{-1}.

LC-MS analyses LC-MS analyses were performed using a Thermo Finnigan LTQ mass spectrometer coupled to a Surveyor HPLC system consisting of a Surveyor Pump Plus, Surveyor PDA Plus and Surveyor Autosampler Plus (Thermo Electron, Waltham, MA, USA). Analyses were performed as described by Alder *et al.* (2008).

Plant material and transformation

Protonemal tissue of wild-type (WT) *Physcomitrella patens*, ecotype Gransden 2004 (Rensing *et al.*, 2008), was grown in liquid or on solid Knop ME medium (Knop medium supplemented with microelements; Horst *et al.*, 2016). Cultivation and protoplast transformation were performed as described before (Frank *et al.*, 2005). Molecular screening of the transgenic lines is described in detail in Methods S1 and S2. For caulonema induction, 5-µl droplets of protonema culture adjusted to 440 mg DW l^{-1} were applied to Knop ME plates. The plates were cultivated under standard conditions for 2 wk and then subjected to darkness in an upright position for another 3 wk. GR24 (Chiralix, Nijmegen, the Netherlands) and carlactone were dissolved in methanol and used with a final concentration of 1 µM. Control plates were treated with methanol only. For experiments with carlactone, the medium was buffered with 5.96 g l^{-1} HEPES and adjusted to pH 7 before sterile filtration. Phosphate starvation experiments were done on Knop ME medium without KH_2PO_4. The medium was buffered with 1 g l^{-1} MES and adjusted to pH 5.8 before sterile filtration. For infection with *Sclerotinia sclerotiorum*, *Physcomitrella* WT and *ΔCCD* mutants were grown in Petri dishes (Ø 9 cm) on a cellophane membrane (400P; Visella Oy, Valkeakoski, Finland) placed on BCD medium (1 mM $MgSO_4$, 1.85 mM KH_2PO_4 (pH 6.5), 10 mM KNO_3, 45 µM $FeSO_4$, 0.22 µM $CuSO_4$, 0.19 µM $ZnSO_4$, 10 µM H_3BO_4, 0.10 µM Na_2MoO_4, 2 µM $MnCl_2$, 0.23 µM $CoCl_2$, 0.17 µM KI) supplemented with 1 mM $CaCl_2$, 45 µM Na_2EDTA and 5 mM ammonium tartrate, and solidified with 0.8% agar. The cultures were grown in a growth chamber at 23°C (photoperiod 12 h, light intensity 50 µmol m^{-2} s^{-1}) and subcultured weekly.

Pathogenicity tests with fungal isolates on *Physcomitrella patens*

Apiospora montagnei (isolate D1), *Fusarium avenaceum* (isolate SS0.1-2), *Fusarium oxysporum* (isolate SSC-1) (Akita *et al.*, 2011), *Irpex* sp. (Lehtonen *et al.*, 2009) and *Sclerotinia sclerotiorum* (a kind gift from H. Li and J. Tuomola, University of Helsinki) were grown on potato dextrose agar (PDA; Biokar Diagnostics, Pantin Cedex, France) at 23°C for 2 wk. Gametophyte tissue of *P. patens* was grown *in vitro* as colonies on BCD medium as described above. To standardize the size of the colonies, a plate full of 1-wk-old protonema was homogenized in 10 ml sterilized 0.25% agar (Sigma), and 70 µl drops of the homogenate were used to initiate six equal-sized moss colonies on a Petri dish. After 4 wk, the moss plates were inoculated by placing a 7-mm diameter agar plug from the fungal cultures in between the moss. GR24 treatment was done as described above. Noninoculated PDA agar plugs were used for control cultures. The fungal growth and severity of infection on moss plates was compared between the WT and *ΔCCD7/8* moss lines. In each experiment, two *ΔCCD8* or three *ΔCCD7* mutant lines were tested as replicates, besides the WT moss included as a control.

Statistical analysis

Statistical analysis was performed using R software (v3.3.0, https://www.R-project.org/). Significance levels of single factor dependency were determined using one-way ANOVA and effect sizes η^2 were calculated from the resulting sums of squares. Significance levels of two factor dependency were determined via linear regression modelling. *Post hoc* pairwise comparison was achieved by comparing least-squares means using the Tukey adjustment for multiple testing.

Results

Physcomitrella CCD7 is a stereospecific 9-*cis*-carotenoid cleavage dioxygenase

A search of the *P. patens* genome (Zimmer *et al.*, 2013) identified the gene Pp3c6_21550 (www.cosmoss.org) as the most closely related to *CCD7* genes of seed plants. The predicted *Physcomitrella* CCD7 protein (ADK36680) showed a similarity of above 60% to those of *Solanum lycopersicon* (NP_001234433) and *Oryza sativa* (NP_001053491). The *Physcomitrella* enzyme consists of 693 amino acids, which is much longer than the CCD7s of seed plants, such as rice and *Arabidopsis* CCD7 that have 609 and 629 amino acids, respectively. Sequence alignment with the aforementioned enzymes revealed that PpCCD7 has an extension at the N-terminus and few short insertions present at different positions of the primary sequence (Fig. S1). Prediction of the transit peptide using ChloroP (Emanuelsson *et al.*, 1999) indicated a transit peptide with 48 amino acids. To avoid negative impact of the transit peptide during *in vitro* enzyme activity assays, we shortened the cloned full-length cDNA to yield a protein without transit peptide. The resulting protein is referred to as PpCCD7.

In order to investigate the activity of PpCCD7 *in vitro*, we expressed the enzyme, encoded in the plasmid pTHIO-DAN1-PpCCD7dTP, in fusion with thioredoxin in BL21(DE3) *E. coli* cells harbouring the vector pGro7, which encodes the chaperones groES-groEL alleviating incorrect folding (Fig. S2). Isolated soluble fractions of PpCCD7 overexpressing cells were then used for *in vitro* assays, in comparison with the corresponding preparation of *Pisum sativum* CCD7-thioredoxin fusion overexpressing cells (Alder *et al.*, 2012), which is referred to here as PsCCD7. In a series of experiments, we tested the conversion of different β-carotene isomers. HPLC analysis showed that PpCCD7 cleaves 9-*cis*-β-carotene at the 9′-10′ double bond resulting in 9-*cis*-β-apo-10′-carotenal and β-ionone, which are also formed by PsCCD7 (Fig. 1a, P1 and P, respectively). Incubation of both enzymes with all-*trans*-, 13-*cis*- and 15-*cis*-β-carotene or other all-*trans*-carotenoids such as all-*trans*-γ-carotene, -cryptoxanthin, -lutein and -zeaxanthin did not lead to any HPLC detectable product (Figs S3, S4). To gain further insight into the substrate specificity of PpCCD7, we produced 9-*cis*-isomers of lutein, zeaxanthin and cryptoxanthin, using iodine, and incubated them with PsCCD7 and PpCCD7. Incubation of PsCCD7 with 9-*cis*-/all-*trans*-zeaxanthin mixture resulted in the

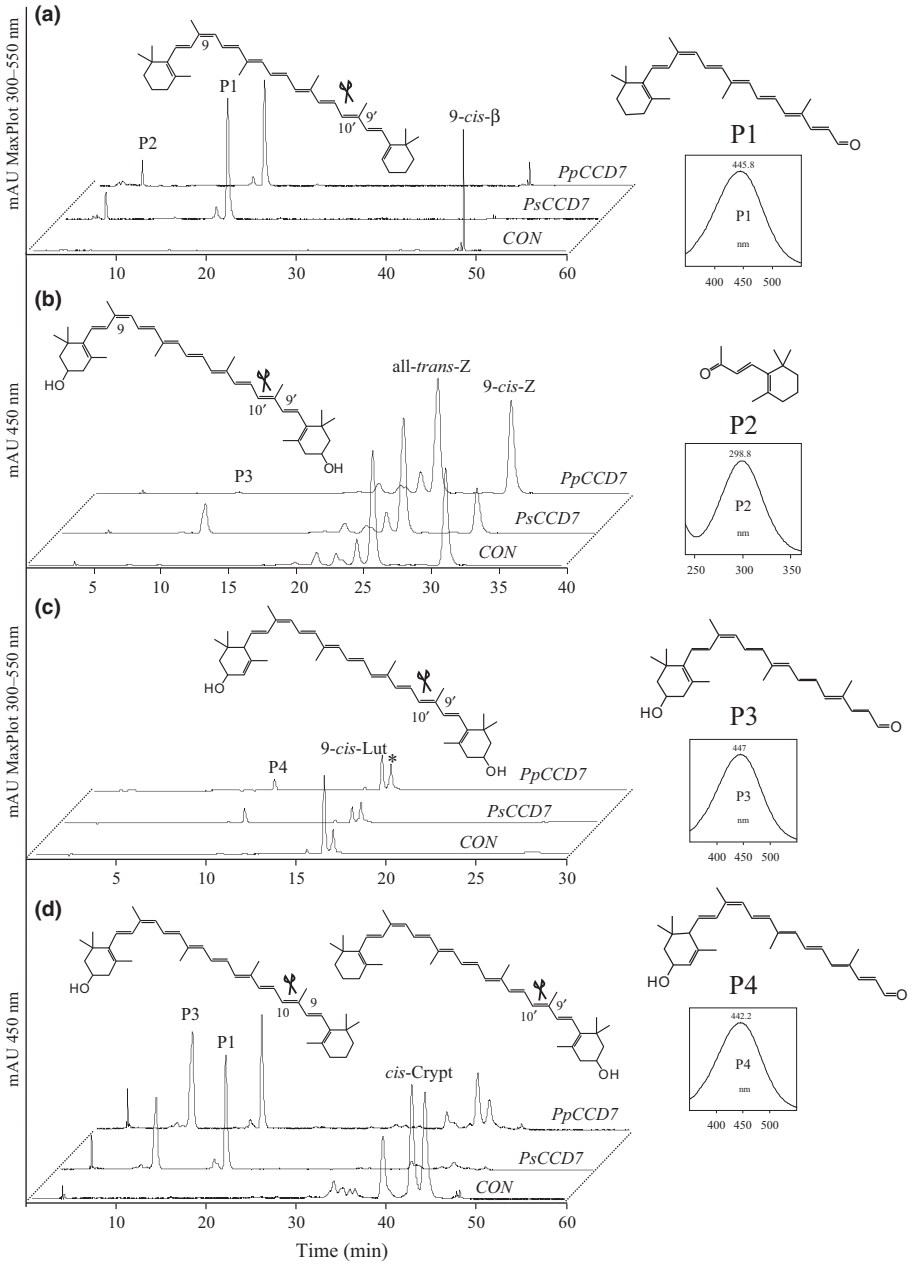

Fig. 1 High performance liquid chromatography (HPLC) analysis of *Physcomitrella patens* carotenoid cleavage dioxygenase 7 (PpCCD7) incubation with different 9-*cis*-carotenoids. The chromatograms show the products obtained with 9-*cis*-β-carotene (a), -zeaxanthin (b), -lutein (c) and both 9- and 9′-*cis*-cryptoxanthin (d). The enzyme converted all substrates into the same products formed by PsCCD7, by cleaving the C9′-C10′ double bond. *, 9′-*cis*-lutein.

formation of 9-*cis*-3-OH-β-apo-10′-carotenal (P3, Fig. 1b) from 9-*cis*-zeaxanthin. The *Physcomitrella* enzyme PpCCD7 showed similar activity, by producing traces of 9-*cis*-3-OH-β-apo-10′-carotenal from the same substrate. Iodine treatment of lutein led to two 9-*cis*-isomers (9-*cis*- and 9′-*cis*-lutein), which show different elution times in the HPLC analysis (Fig. 1c). PsCCD7 and PpCCD7 converted the earlier eluting isomer into product P4 (Fig. 1c). Absorption maximum and elution time of P4 indicated that it is a 9-*cis*-3-OH-α-apo-10′-carotenal expected to arise by cleaving the 9-*cis*-lutein isomer carrying the *cis* double bond next to the 3-OH-β-ionone ring (cleavage position is depicted in Fig. 1c). Cryptoxanthin can also occur as a 9-*cis*- and a 9′-*cis*-isomer that differ in the position of the *cis*-double-bond relative to the β-ionone or 3-OH-β-ionone ring (Fig. 1d). As shown in the HPLC analysis (Fig. 1d), the two enzymes converted both isomers, yielding P1 (9-*cis*-3-β-apo-10′-carotenal) and P3 (9-*cis*-3-OH-β-apo-10′-carotenal), suggesting the cleavage of the C9′-C10′/C9-C10 double bond. The identity of P1, P3 and that of 3-OH-β-ionone, the second product of the 9′-*cis*-cryptoxanthin cleavage, were confirmed by LC-MS (Fig. S5).

Physcomitrella CCD8 is a carlactone synthase

In order to test the enzymatic activity of PpCCD8 (Pp3c6_21520, ADK36681; Proust *et al.*, 2011), we cloned the corresponding cDNA and generated the plasmid pTHIO-DAN3-PpCCD8 encoding a thioredoxin-PpCCD8 fusion. We then expressed the fusion protein in the *E. coli* strain described above (Fig. S2) and incubated soluble fractions of overexpressing cells. Here again, we used the corresponding preparation of the

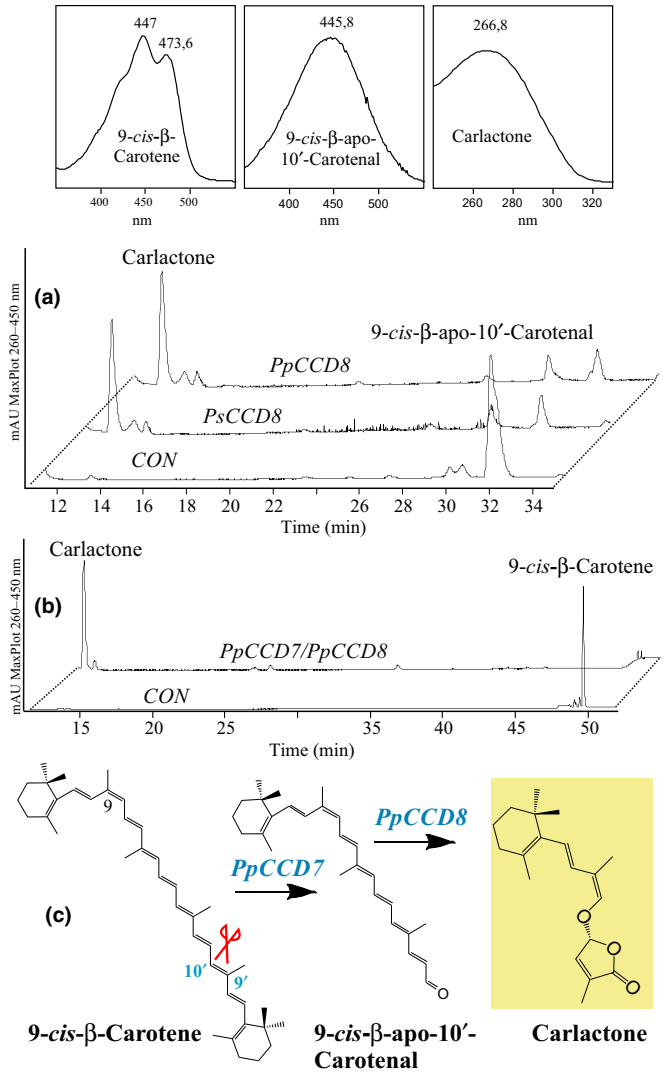

Fig. 2 High performance liquid chromatography (HPLC) analysis of *Physcomitrella patens* carotenoid cleavage dioxygenase 8 (PpCCD8) activity. The chromatograms show the conversion of 9-*cis*-β-apo-10′-carotenal by PpCCD8 and PsCCD8 into carlactone (a) that was also produced upon incubation of 9-*cis*-β-carotene with PpCCD7/PpCCD8 and PsCCD7/PsCCD8 (b). (c) The scheme depicts the steps leading to carlactone from 9-*cis*-β-carotene. UV-Vis spectra of substrates and carlactone are depicted in the insets above.

pea enzyme PsCCD8, encoded in pThio-Ps8 (Alder *et al.*, 2008), for comparison.

In a first approach, we incubated PpCCD8 with 9-*cis*-β-apo-10′-carotenal and analysed the assay by HPLC. As shown in Fig. 2(a), PpCCD8 converted this substrate into a compound identical to carlactone produced by PsCCD8 in retention time and UV-Vis spectral properties. Combined incubation of PpCCD7 and PpCCD8 with 9-*cis*-β-carotene also led to carlactone (Fig. 2b), suggesting that *Physcomitrella* employs the same pathway as seed plants to produce this compound (Fig. 2c). CCD8s from rice, pea and *Arabidopsis* show a dual activity in cleaving all-*trans*-β-apo-10′-carotenal/ol besides 9-*cis*-β-apo-10′-carotenal (Alder *et al.*, 2008, 2012). Therefore, we tested the cleavage of all-*trans*-β-apo-10′-carotenal/ol by PpCCD8 and found that the enzyme converted this substrate by cleaving the C13,C14-double bond, leading to β-apo-13-carotenone (Fig. S6), as shown for CCD8 enzymes of seed plants. We further tested the cleavage of C_{40}-carotenoids by incubating the enzymes with all-*trans*-zeaxanthin, -β-carotene, -γ-carotene and -cryptoxanthin, and with 9-*cis*-configured carotenoids. However, none of the incubations with all-*trans* (Fig. S7) and 9-*cis*-C_{40} carotenoids led to any HPLC-detectable conversion (Fig. S8). These data suggest that PpCCD8 is a stereospecific apocarotenal cleavage dioxygenase and a carlactone synthase.

Physcomitrella ΔCCD7 mutants show enhanced caulonema growth

In order to elucidate the biological function of PpCCD7 and pPCCD8, *ΔCCD7* and *ΔCCD8* knockout lines were generated and confirmed as clear gene knockouts as they did not show any transcript of *CCD7* and *CCD8*, respectively, in reverse transcription polymerase chain reaction analyses (Fig. S9). Based on Southern Blot results (Fig. S10), the lines *ΔCCD7*-17, -21 and -23, as well as *ΔCCD8*-15 and -18, were chosen for further analyses. These lines were stored in the International Moss Stock Center under the accession numbers given in Table S2.

When transferred to darkness, *Physcomitrella* develops caulonema filaments that originate from chloronemal tip cells. Compared to WT, *ΔCCD7* and *ΔCCD8* lines formed more and longer filaments (Fig. 3a–c). A similar observation was made previously with a *ΔCCD8* mutant (Hoffmann *et al.*, 2014), however, the phenotype seems to be more pronounced under the conditions used in the present study. The filaments of 5–15 colonies from each genotype were counted after 32 d in darkness. The average number of caulonema filaments was > 20 for the WT (24.8 ± 4.7) and > 80 for the *ΔCCD7* (84.9 ± 8.1) and *ΔCCD8* (81.7 ± 8.9) lines, respectively. The number of caulonema filaments mirrors the higher branching grade of the mutant protonemata, which was observed before and which is already determined before switching to growth in darkness. The length of *ΔCCD* caulonema filaments was nearly doubled compared to WT (WT 9.9 ± 1.6 mm, *ΔCCD7* 18.0 ± 2.0 mm, *ΔCCD8* 17.6 ± 1.8 mm). This increase in filament length was caused by an increased cell number rather than increased cell length. The number of cells in *ΔCCD* filaments was doubled compared to WT cell numbers (WT 19.8 ± 2.6, *ΔCCD7* 41.3 ± 2.9, *ΔCCD8* 40.8 ± 2.9; Fig. 3d).

Rescue of *ΔCCD7* and *ΔCCD8* phenotypes by carlactone and GR24

Hoffmann *et al.* (2014) reported that treatment with GR24 and natural SLs rescued the caulonema phenotype of the *ΔCCD8* mutant. Our complementation experiments were performed with six colonies of the different *ΔCCD7* and *ΔCCD8* lines, respectively, and 15 colonies of WT. Treatment with GR24 resulted in WT-like growth regarding filament number as well as filament length under caulonema-inducing conditions after 3 wk in

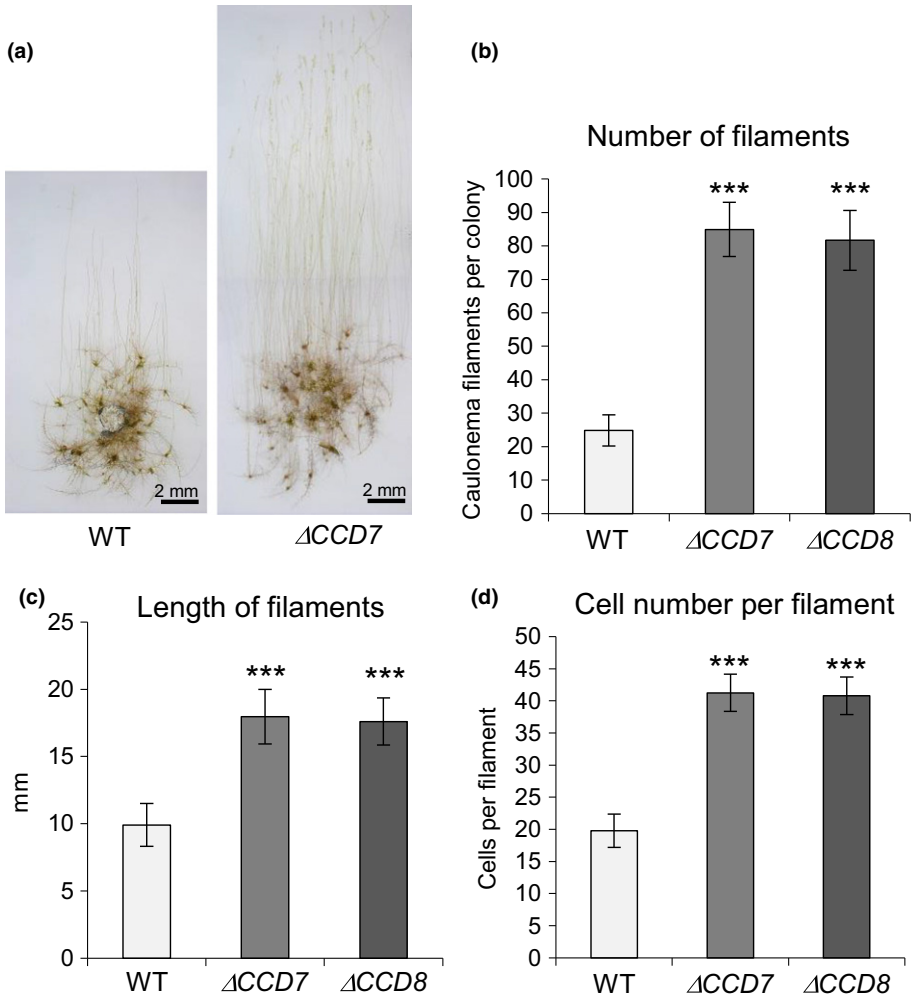

Fig. 3 Knockout of *Physcomitrella patens* carotenoid cleavage dioxygenases *PpCCD7* and *PpCCD8* leads to an increased number and length of caulonema filaments in *Physcomitrella patens*. (a) Examples of a *ΔCCD7* colony and a wild-type (WT) colony after 3 wk of growth in darkness. Number (b) and length of caulonema filaments (c) are significantly increased in *ΔCCD7* and *ΔCCD8* compared to WT. (d) The increased length observed is caused by an increase in cell numbers. The numbers of colonies measured were five for WT, 15 for *ΔCCD7* and 10 for *ΔCCD8*; the filaments measured 10 for WT, 30 for *ΔCCD7* and 20 for *ΔCCD8*; the filaments from which cell numbers were counted were five for WT, 15 for *ΔCCD7* and 10 for *ΔCCD8*. ***, $P < 0.001$, one-way ANOVA followed by a pairwise comparison with Tukey's adjustment. Error bars represent standard deviation (± SD) from the mean.

darkness (Fig. 4a,b). Only very few caulonema filaments per colony were formed in all lines kept on GR24-containing medium (WT 1.6 ± 1.7, *ΔCCD7* 3.2 ± 2.8, *ΔCCD8* 1.0 ± 0.7). Also, the length of the filaments decreased severely to similar levels for all lines (WT 2.0 ± 1.0 mm, *ΔCCD7* 2.4 ± 1.5 mm, *ΔCCD8* 1.7 ± 0.8 mm). Next, we aimed to test whether application of carlactone also can restore the WT caulonema phenotype in *ΔCCD7* and *ΔCCD8* lines. As carlactone is unstable in physiological (acid) pH, we used a growth medium buffered to an increased pH value of pH 7, to enhance the stability of carlactone. However, the increase and control of pH had a general stimulating effect on caulonema formation in the analysed *Physcomitrella* lines, and therefore the differences between WT and *ΔCCD* mutants were not as pronounced as in pH 5.8 which is the physiological pH for *Physcomitrella* cultivation and was used in all other experiments. Nevertheless, adding carlactone to the growth medium led to a partial rescue of the knockout phenotypes (Fig. 4c,d). Although *ΔCCD* mutants had twice as many caulonema filaments as the WT on carlactone-free growth medium (WT 105.7 ± 16.5, *ΔCCD7* 217.2 ± 16.0, *ΔCCD8* 215.5 ± 12.7), numbers of filaments dropped to near WT levels (WT 90.2 ± 16.8, *ΔCCD7* 126.2 ± 19.1, *ΔCCD8* 132.1 ± 11.3, Fig. 4c) and the effect of the mutant lines on the number of filaments decreased considerably on carlactone-containing growth medium (effect size $\eta^2 = 0.92$ without carlactone, $\eta^2 = 0.56$ with carlactone). The length of filaments was 11.3 ± 3.2 mm for WT, 18.3 ± 2.3 mm for *ΔCCD7* and 18.0 ± 2.3 mm for *ΔCCD8* on the medium buffered to pH 7. When carlactone was added to the medium, the length of WT filaments stayed nearly the same (12.0 ± 2.3 mm), whereas the length of *ΔCCD7* and *ΔCCD8* filaments decreased to 14.0 ± 2.3 mm and 14.7 ± 2.1 mm, respectively, corresponding to the decrease of the mutant effect observed in the number of filaments (effect size $\eta^2 = 0.36$ without carlactone, $\eta^2 = 0.18$ with carlactone; Fig. 4d). These data confirm that the observed mutant phenotypes are caused by SL deficiency that results from the lack of CCD7 or CCD8 activity, and indicate that *Physcomitrella* SL biosynthesis proceeds via carlactone.

ΔCCD7 exudates have reduced seed germination activity

In order to test whether SLs produced by *Physcomitrella* can induce seed germination in root-parasitic plants and to determine whether the absence of CCD7 or CCD8 had an impact on SL release, a germination assay was carried out with *Orobanche ramosa* seeds (Fig. 5). For this purpose, seeds were placed in the

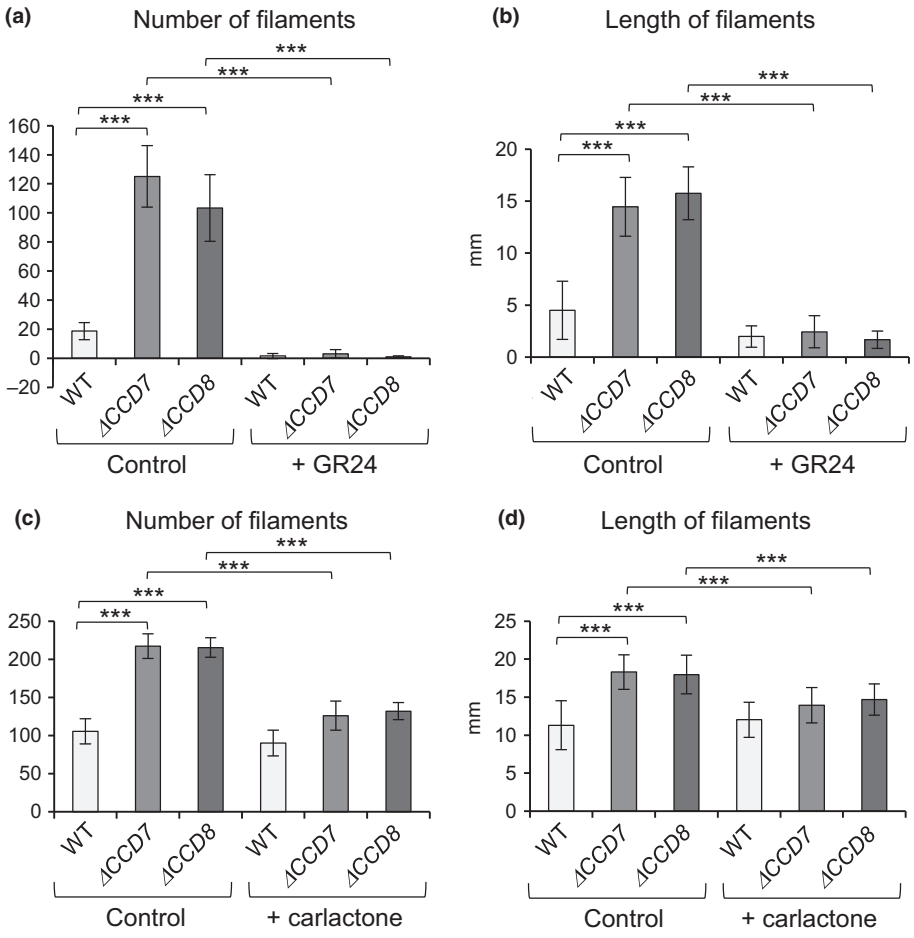

Fig. 4 GR24 and carlactone application affected the number and length of caulonema filaments in *Physcomitrella patens* carotenoid cleavage dioxygenases *ΔCCD7* and *ΔCCD8* mutants. Addition of 1 μM GR24 to the growth medium (a, b), addition of 1 μM carlactone to the growth medium (c, d). Numbers and length of untreated *ΔCCD7* and *ΔCCD8* caulonema filaments differed significantly from wild-type (WT) and treated mutants (***, $P < 0.001$, multiple pairwise comparisons, using least squares means and Tukey's adjustment). Error bars represent standard deviation (± SD) from the mean.

vicinity of WT and knockout plants (between 139 and 455 seeds per plate; see Table S3), and germination was measured by visual inspection (Fig. 5b–e). Because growth under phosphate shortage triggers SL production and release in seed plants (Yoneyama *et al.*, 2012), germination under normal and phosphate-starvation conditions was compared. As a positive control, a plate containing 1 μM of GR24 was used. Seed germination on *Physcomitrella* WT plates was 16% on standard growth medium and increased to 39% under phosphate starvation, whereas the germination rate on the GR24-containing positive controls was 59%. By contrast, no seeds germinated when placed on *ΔCCD7* or *ΔCCD8* plates. However, in a pre-experiment using four of the *ΔCCD7* lines and another lot of *Orobanche* seeds, we observed a very low germination activity (< 1.5%) on *ΔCCD7* plates (Fig. S11). These data suggest that *Physcomitrella* releases carlactone-derived, SLs/related compounds that are effective to trigger seed germination of root-parasitic plants. This process is regulated by phosphate availability, similar to what was described for seed plants and was abolished in *ΔCCD7* and *ΔCCD8* lines.

ΔCCD7 and *ΔCCD8* mutants show an enhanced susceptibility to fungal infection

It was recently shown that knocking down the *CCD8* expression increased the susceptibility of tomato to fungal pathogens (Torres-Vera *et al.*, 2014). Therefore, we tested the susceptibility of *ΔCCD7* and *ΔCCD8* mutants to the phytopathogenic fungi *Apiospora montagnei*, *Fusarium avenaceum*, *Fusarium oxysporum*, *Irpex* sp. and *Sclerotinia sclerotiorum* over a period of 9 d post infection (dpi). Upon infestation with *Sclerotinia sclerotiorum* (Fig. 6a), *F. oxysporum* (Fig. S12) and *Irpex* sp. (Fig. S13), moss plants lacking CCD7 or CCD8 showed earlier and more severe disease symptoms than the WT. These differences were less pronounced in colonies infested by *Apiospora montagnei* and *F. avenaceum* (data not shown). Because the infection with *S. sclerotiorum* led to the most obvious differences in disease symptoms, we tested whether the enhanced susceptibility to this fungus is a result of SL deficiency. For this purpose, we performed the *S. sclerotiorum* pathogenicity study in the presence of the SL analogue GR24 (at 1 μM concentration). As shown in Fig. 6(b), the application of GR24 restored the resistance of *ΔCCD7* and *ΔCCD8* plants to the fungus as long as 18 dpi. Moreover, the application of GR24 increased the resistance of mutants and WT plants to the fungus (Fig. 6b, first and third column), suggesting a contribution of SLs to plant resistance against fungal infection. Whether the weaker disease symptoms observed upon adding GR24 were caused by a direct toxic effect of this compound to the fungus or by a decreased susceptibility of the moss lines to *S. sclerotiorum* infection was tested by determining the growth rate of this fungus in the presence of different

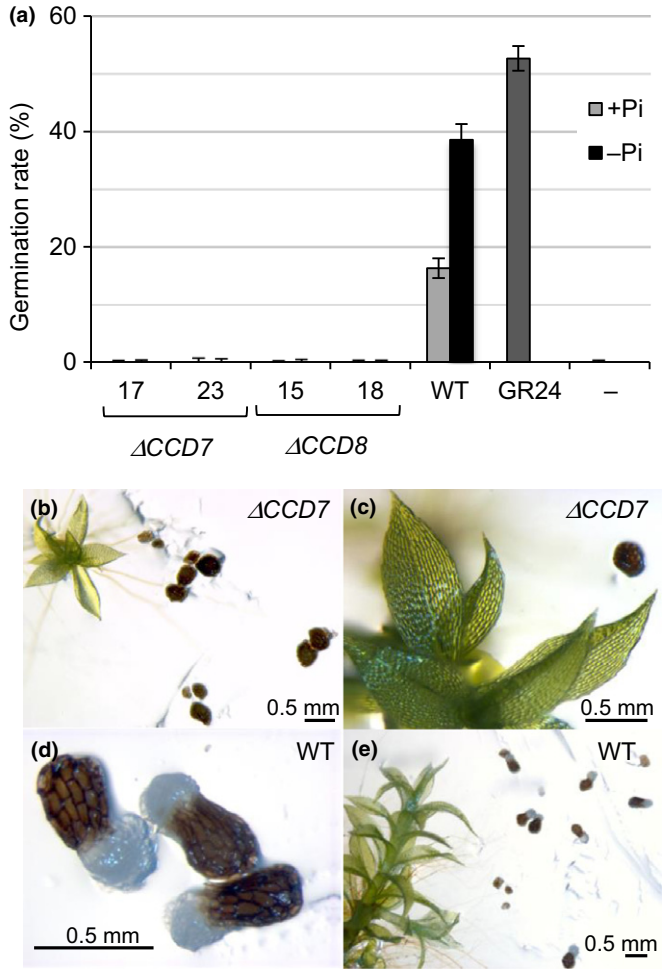

Fig. 5 Effect of wild-type (WT) and carotenoid cleavage dioxygenase *ΔCCD7* mutant on the germination of *Orobanche ramosa* seeds. (a) Germination rates of *O. ramosa* seeds on plates with *Physcomitrella patens* WT, *ΔCCD7* (17, 23) and *ΔCCD8* (15, 18) lines under standard conditions (+Pi) and phosphate starvation conditions (−Pi); positive control: GR24 (1 μM); negative control: solvent; error bars indicate the statistical uncertainty. *O. ramosa* seeds on plates with *ΔCCD7* (b, c) and WT (d, e). The protruding radicle is visible in germinated seeds.

GR24 concentrations between 5 and 50 μM (Fig. S14; Methods S3). We observed a slightly nonlinear growth of *Sclerotinia* (Fig. S14a), which was not affected by 5 μM GR24. To particularize this effect, we calculated the percentage of growth inhibition for each GR24 concentration and time point (Fig. S14b), and assessed the colony growth macroscopically (Fig. S14c). GR24 concentrations of 10 and 15 μM reduced the *Sclerotinia* colony size by *c.* 10% compared to the control. Growth was inhibited by *c.* 20% at a GR24 concentration of 25 μM and increased up to 50% at 50 μM of GR24 in the medium. These data are in line with the report of Dor *et al.* (2011) and demonstrate that the growth-inhibiting effect of GR24 occurs at much higher concentrations than the one used in the infection experiment (1 μM), and indicate that the milder *Sclerotinia* infection symptoms of *Physcomitrella* WT and *ΔCCD7* and *ΔCCD8* mutants, which were observed in the presence of 1 μM GR24, are caused by increased plant resistance rather than a direct effect of GR24 on the growth of the fungus.

Discussion

Strigolactones (SLs) are unstable and produced at very low concentrations. Both characteristics impede their detection and identification. Therefore, using *in vitro* assays with putative biosynthetic enzymes and available substrates is a fruitful approach to trace the presence of these compounds and to shed light on their biosynthesis and evolution. In seed plants, the two carotenoid cleavage dioxygenases CCD7 and CCD8 have been shown to catalyse the conversion of 9-*cis*-β-carotene into carlactone, via the intermediate 9-*cis*-β-apo-10′-apocarotenal (Alder *et al.*, 2012; Bruno *et al.*, 2014). Carlactone is then converted by the cytochrome P450 clade 711, more axillary growth 1 (MAX1), and homologues into carlactonoic acid and the canonical strigolactone 4-deoxyorobanchol (Abe *et al.*, 2014; Zhang *et al.*, 2014). The genome of the early diverging land plant *Physcomitrella patens* encodes a putative CCD7 (PpCCD7) and a putative CCD8 (PpCCD8), but no obvious MAX1 homologues (Zimmer *et al.*, 2013). The absence of MAX1 prompted us to investigate the enzymatic activities of the *Physcomitrella* CCD7 and CCD8 and to check whether the combination of these enzymes also leads to carlactone.

Our data show that PpCCD7 catalyses the cleavage of the C9–C10-double bond in various carotenoids, including β-carotene, zeaxanthin, lutein and cryptoxanthin, yielding the corresponding apo-10′-carotenal (C_{27}), that is β-apo-10′-carotenal, and C_{13}-ketone (β-ionone). However, the enzyme only cleaved the 9-*cis*-configured isomers of the tested substrates and produced 9-*cis*-configured C_{27}-product(s), demonstrating its stereo-selectivity and its role in providing CCD8 with the suitable stereoisomer for carlactone formation. Thus, PpCCD7 resembles homologues from seed plants in its stereo-specificity and the relatively wide range of converted 9-*cis*-configured substrates (Bruno *et al.*, 2014). Interestingly, PpCCD8 *in vitro* showed the same dual activity reported for CCD8 from rice, pea and *Arabidopsis* (Alder *et al.*, 2008, 2012). PpCCD8 converted both 9-*cis*-β-apo-10′-carotenal and all-*trans*-β-apo-10′-carotenal, leading to carlactone and β-apo-13-carotenone, respectively. Although carlactone has an established role as the precursor of SLs (Abe *et al.*, 2014; Seto *et al.*, 2014; Zhang *et al.*, 2014), the biological significance of β-apo-13-carotenone formation is still elusive.

Our data demonstrate that the pathways for converting 9-*cis*-β-carotene to carlactone are evolutionarily conserved between *Physcomitrella* and seed plants. Moreover, it can be assumed that *Physcomitrella* utilizes DWARF27 to produce the correctly configured stereoisomer that is then cleaved by CCD7. Indeed, several DWARF27 homologues are encoded by the *Physcomitrella* genome (Zimmer *et al.*, 2013). The conversion of hydroxylated carotenoids, such as 9-*cis*-lutein, by PpCCD7 opens up the possibility of forming SLs that do not originate from β-carotene. An example of such compounds is heliolactone that supposedly derives from an ε-ring-containing precursor, for example α-carotene or lutein (Ueno *et al.*, 2014). However, the synthesis

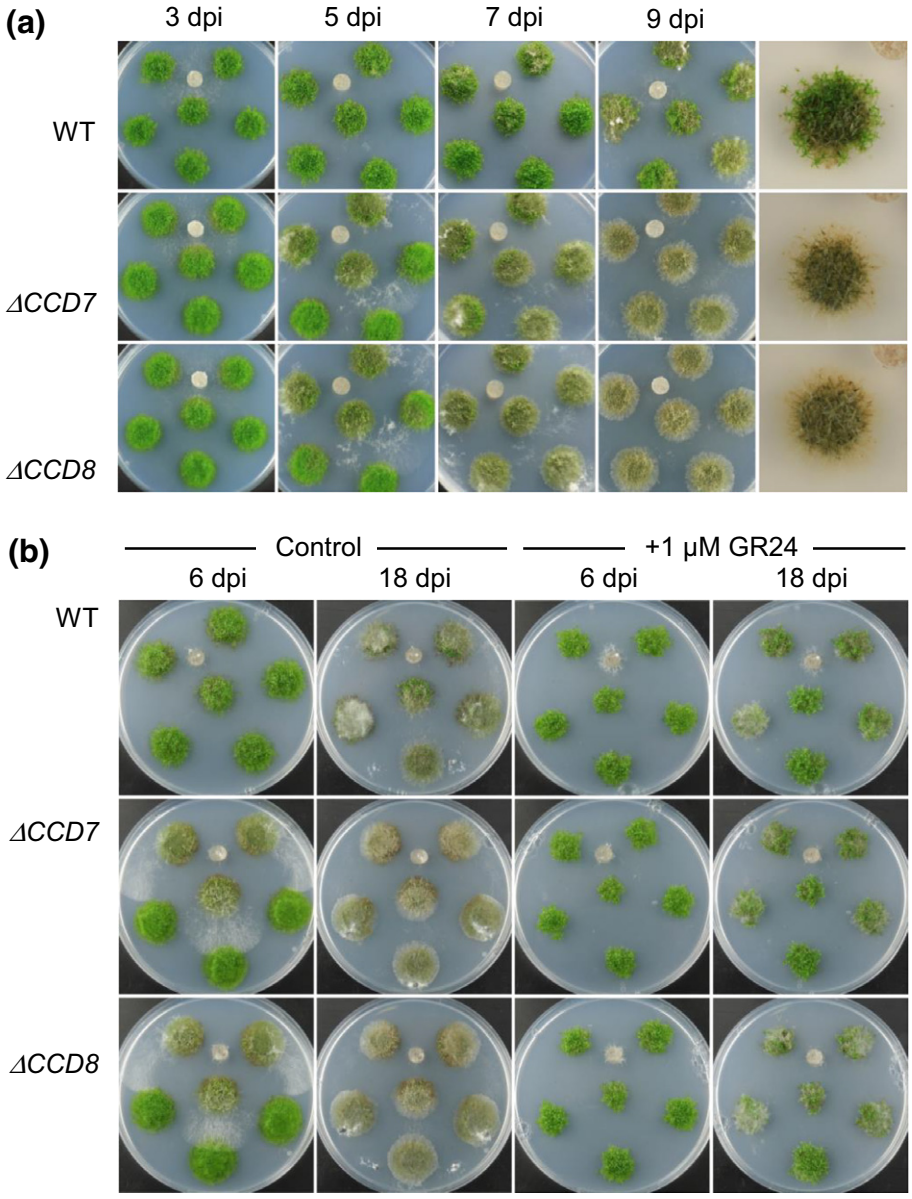

Fig. 6 Susceptibility of *Physcomitrella patens* wild-type (WT) and carotenoid cleavage dioxygenase *ΔCCD7* and *ΔCCD8* mutants to infection with *Sclerotinia sclerotiorum*. (a) Development of symptoms 3, 5, 7 and 9 d post infection (dpi) in WT moss (upper row) and mutants *ΔCCD7* (middle row) and *ΔCCD8* (lower row). The magnified photographs of moss colonies to the right represent the average severity of disease symptoms in WT and mutants, respectively. (b) Influence of the strigolactone analogue GR24 (1 μM) in the growth medium on the severity of symptoms caused by *Sclerotinia sclerotiorum* in WT (upper row) and mutants *ΔCCD7* (middle row) and *ΔCCD8* (lower row). Columns 1 and 2 display symptoms 6 and 18 dpi, respectively, for moss colonies on standard medium, whereas columns 3 and 4 display the symptoms in moss colonies growing on GR24-containing media 6 and 18 dpi, respectively.

of such SLs requires the conversion of the CCD7 products by CCD8 and the formation of structures such as 3-OH-carlactone or α-carlactone.

It can be assumed that *Physcomitrella* produces carlactone, as suggested by its formation by sequential action of PpCCD7 and PpCCD8 *in vitro* and its activity in rescuing the *ΔCCD7* and *ΔCCD8* phenotype. However, the question of how carlactone is converted into canonical SLs remains open because of the lack of obvious MAX1 homologues in *Physcomitrella*. Proust *et al.* (2011) reported on the presence of different SLs in WT *Physcomitrella*, including strigol, fabacyl acetate, orobanchol and different orobanchol derivatives. However, we could not detect SLs, such as orobanchol and deoxystrigol, in *Physcomitrella*. Therefore, we relied on seed germination of *Orobanche ramosa* as a sensitive bioassay to test the presence of SLs and related compounds with SL-like activity in the vicinity of moss colonies. Our results prove that *Physcomitrella* releases compounds that induce seed germination in this root-parasitic weed and that CCD7 and CCD8 are required for the synthesis of these compounds. Placed on *Physcomitrella* wild-type (WT) plates, *Orobanche* seeds germinated to 73% of the extent as on GR24-containing control medium, whereas germination was abolished on *ΔCCD7* and *ΔCCD8* plates. This may indicate that SLs described for a *ΔCCD8* knockout before (Proust *et al.*, 2011) are of no relevance for *Orobanche* germination. Residual activity, which we observed in other experiments with a different seed batch, may indicate the presence of other – non-SL – compounds with seed-germinating activity in *ΔCCD7* lines. Alternatively, one might speculate about the presence of an alternative route for SL biosynthesis with a small contribution to the overall SL content. This possibility was suggested previously (de Saint Germain *et al.*, 2013) and might be supported by the earlier report on the presence of strigol and fabacyl acetate in

ΔCCD8 mutants of pea and moss (Foo & Davies, 2011; Proust *et al.*, 2011).

An intensively studied aspect of SL function is the regulation of shoot branching (Gomez-Roldan *et al.*, 2008; Umehara *et al.*, 2008; reviewed in Waldie *et al.*, 2014). Our SL biosynthesis-deficient *ΔCCD7* and *ΔCCD8* mutants showed increased protonema branching resembling the shoot-branching phenotypes of SL biosynthesis and signalling mutants of seed plants. Enhanced branching in a moss *ΔCCD8* mutant was reported for the juvenile protonema tissue and the adult moss 'shoots', the gametophores (Proust *et al.*, 2011; Coudert *et al.*, 2015), and was reduced by cultivation on GR24-containing medium (Hoffmann *et al.*, 2014; Coudert *et al.*, 2015). This is analogous to our results from caulonema filament-inducing growth conditions. We observed increased branching in protonema tissue, deduced from the more than doubled number of filaments in *ΔCCD7* and *ΔCCD8* mutants compared to WT. Branching of all lines was heavily suppressed by GR24 treatment, but also reduced to WT-like numbers by treatment with the SL precursor carlactone.

Our data presented here are in accordance with the proposed hypothesis of a general function for SLs in regulating the plant's response to environmental cues, which arose from the dramatic changes that plants underwent during their conquest of land, for example limited nutrient availability (Brewer *et al.*, 2013). Phosphate deprivation was shown to increase SL production in seed plants, which in turn induces hyphal branching of arbuscular mycorrhiza (Yoneyama *et al.*, 2007, 2015; Kapulnik & Koltai, 2016). Employing the *Orobanche* seed germination bioassay, we detected a clear response of WT *Physcomitrella* to phosphate-starvation growth conditions. Depleting phosphate led to a striking increase in the ratio of germinating seeds, indicating largely increased SL exudation as a response to phosphate shortage.

An additional aspect of coping with suboptimal conditions is to control the numerous biotic competitors colonizing the moist habitats of bryophytes. For a long time, bryophytes have been used in traditional medicine because of their ascribed antimicrobial effects (Beike *et al.*, 2010). Here, we demonstrated the modulation of susceptibility to infection by the pathogenic fungus *Sclerotinia sclerotiorum* depending on SL availability. Although the SL-deficient *ΔCCD7* and *ΔCCD8* mutants were more susceptible to fungal infection, treatment with the SL analogue GR24 conferred increased resistance not only to the *ΔCCD7* and *ΔCCD8* mutants, but also to the WT. This effect was evidently not caused by a direct growth inhibition, which occurred only under much higher GR24 concentrations, but a positive modulation of plant defence mechanisms induced by the SL compound. Previously, studies utilizing gene knockout mutants of *P. patens* have pinpointed a peroxidase that plays an important role in resistance to fungi in *P. patens* (Lehtonen *et al.*, 2009). The role of SL in pathogen defence of *P. patens* discovered in the present study provides another example of the disease resistance mechanisms in bryophytes, which are still poorly understood at the genetic level.

Our results reveal the deep evolutionary conservation of SL biosynthesis, SL function, and its regulation by biotic and abiotic cues. They thus suggest that this system has evolved in the last common ancestor of mosses and seed plants, and may have facilitated the conquest of land by plants.

Acknowledgements

We thank Harro Bouwmeester and Carolien Ruyter-Spira for valuable discussions, Agnes Novakovic for supporting the generation and analysis of *ΔCCD* lines, and Anne Katrin Prowse for editing the language of the manuscript. This work was supported by the Deutsche Forschungsgemeinschaft (DFG; grant AL892/1-4 and the Graduiertenkolleg 1305 'Plant Signal Systems'), King Abdullah University of Science and Technology (KAUST; baseline funding of S.A-B.), the Excellence Initiative of the German Federal and State Governments (grant no. EXC 294 BIOSS to R.R.), and The Academy of Finland (grant 1253126 to J.P.T.V.).

Author contributions

S.A-B., E.L.D. and R.R. planned and designed the research; A.A., S.H., J.F., B.S., K.L.K., S.N., G.W., V.S-R., M.T.L., A.B. and L.B. performed experiments and analysed data; and S.A-B., E.L.D., J.P.T.V. J.A. and R.R. wrote the manuscript. All authors discussed data and approved the final version of the manuscript.

References

Abe S, Sado A, Tanaka K, Kisugi T, Asami K, Ota S, Kim HI, Yoneyama K, Xie X, Ohnishi T *et al.* 2014. Carlactone is converted to carlactonoic acid by MAX1 in *Arabidopsis* and its methyl ester can directly interact with AtD14 *in vitro*. *Proceedings of the National Academy of Sciences, USA* **111**: 18084–18089.

Akita M, Lehtonen MT, Koponen H, Marttinen EM, Valkonen JP. 2011. Infection of the Sunagoke moss panels with fungal pathogens hampers sustainable greening in urban environments. *Science of the Total Environment* **409**: 3166–3173.

Akiyama K, Matsuzaki K, Hayashi H. 2005. Plant sesquiterpenes induce hyphal branching in arbuscular mycorrhizal fungi. *Nature* **435**: 824–827.

Al-Babili S, Bouwmeester HJ. 2015. Strigolactones, a novel carotenoid-derived plant hormone. *Annual Review of Plant Biology* **66**: 161–186.

Alder A, Holdermann I, Beyer P, Al-Babili S. 2008. Carotenoid oxygenases involved in plant branching catalyse a highly specific conserved apocarotenoid cleavage reaction. *The Biochemical Journal* **416**: 289–296.

Alder A, Jamil M, Marzorati M, Bruno M, Vermathen M, Bigler P, Ghisla S, Bouwmeester H, Beyer P, Al-Babili S. 2012. The path from β-carotene to carlactone, a strigolactone-like plant hormone. *Science* **335**: 1348–1351.

Arite T, Iwata H, Ohshima K, Maekawa M, Nakajima M, Kojima M, Sakakibara H, Kyozuka J. 2007. DWARF10, an RMS1/MAX4/DAD1 ortholog, controls lateral bud outgrowth in rice. *Plant Journal* **51**: 1019–1029.

Auldridge ME, McCarty DR, Klee HJ. 2006. Plant carotenoid cleavage oxygenases and their apocarotenoid products. *Current Opinion in Plant Biology* **9**: 315–321.

Beike AK, Decker EL, Frank W, Lang D, Vervliet-Scheebaum M, Zimmer AD, Reski R. 2010. Applied bryology – bryotechnology. *Tropical Bryology* **31**: 22–32.

Beike AK, Lang D, Zimmer AD, Wüst F, Trautmann D, Wiedemann G, Beyer P, Decker EL, Reski R. 2015. Insights from the cold transcriptome of *Physcomitrella patens*: global specialization pattern of conserved transcriptional regulators and identification of orphan genes involved in cold acclimation. *New Phytologist* **205**: 869–881.

Bennett TA, Liu MM, Aoyama T, Bierfreund NM, Braun M, Coudert Y, Dennis RJ, O'Connor D, Wang XY, White CD *et al.* 2014. Plasma

membrane-targeted PIN proteins drive shoot development in a moss. *Current Biology* **24**: 2776–2785.

Besserer A, Bécard G, Jauneau A, Roux C, Séjalon-Delmas N. 2008. GR24, a synthetic analog of strigolactones, stimulates the mitosis and growth of the arbuscular mycorrhizal fungus *Gigaspora rosea* by boosting its energy metabolism. *Plant Physiology* **148**: 402–413.

Bierfreund NM, Tintelnot S, Reski R, Decker EL. 2004. Loss of GH3 function does not affect phytochrome- mediated development in a moss, *Physcomitrella patens*. *Journal of Plant Physiology* **161**: 823–835.

Bitrián M, Roodbarkelari F, Horváth M, Koncz C. 2011. BAC-recombineering for studying plant gene regulation: developmental control and cellular localization of SnRK1 kinase subunits. *Plant Journal* **65**: 829–842.

Booker J, Auldridge M, Wills S, McCarty D, Klee H, Leyser O. 2004. MAX3/CCD7 is a carotenoid cleavage dioxygenase required for the synthesis of a novel plant signaling molecule. *Current Biology* **14**: 1232–1238.

Booker J, Sieberer T, Wright W, Williamson L, Willett B, Stirnberg P, Turnbull C, Srinivasan M, Goddard P, Leyser O. 2005. *MAX1* encodes a cytochrome P450 family member that acts downstream of *MAX3/4* to produce a carotenoid-derived branch-inhibiting hormone. *Developmental Cell* **8**: 443–449.

Bouvier F, Isner J-C, Dogbo O, Camara B. 2005. Oxidative tailoring of carotenoids: a prospect towards novel functions in plants. *Trends in Plant Science* **10**: 187–194.

Brewer PB, Koltai H, Beveridge CA. 2013. Diverse roles of strigolactones in plant development. *Molecular Plant* **6**: 18–28.

Brewer PB, Yoneyama K, Filardo F, Meyers E, Scaffidi A, Frickey T, Akiyama K, Seto Y, Dun EA, Cremer JE *et al.* 2016. *LATERAL BRANCHING OXIDOREDUCTASE* acts in the final stages of strigolactone biosynthesis in Arabidopsis. *Proceedings of the National Academy of Sciences, USA* **113**: 6301–6306.

Bruno M, Al-Babili S. 2016. On the substrate specificity of the rice strigolactone biosynthesis enzyme DWARF27. *Planta* **243**: 1429–1440.

Bruno M, Hofmann M, Vermathen M, Alder A, Beyer P, Al-Babili S. 2014. On the substrate- and stereospecificity of the plant carotenoid cleavage dioxygenase 7. *FEBS Letters* **588**: 1802–1807.

Cook CE, Whichard LP, Turner B, Wall ME, Egley GH. 1966. Germination of witchweed (*Striga lutea* Lour.): isolation and properties of a potent stimulant. *Science* **154**: 1189–1190.

Coudert Y, Palubicki W, Ljung K, Novak O, Leyser O, Harrison CJ. 2015. Three ancient hormonal cues co-ordinate shoot branching in a moss. *eLife* **4**: e06808.

Delaux P-M, Xie X, Timme RE, Puech-Pages V, Dunand C, Lecompte E, Delwiche CF, Yoneyama K, Bécard G, Séjalon-Delmas N. 2012. Origin of strigolactones in the green lineage. *New Phytologist* **195**: 857–871.

Dor E, Joel DM, Kapulnik Y, Koltai H, Hershenhorn J. 2011. The synthetic strigolactone GR24 influences the growth pattern of phytopathogenic fungi. *Planta* **234**: 419–427.

Drummond RSM, Martínez-Sánchez NM, Janssen BJ, Templeton KR, Simons JL, Quinn BD, Karunairetnam S, Snowden KC. 2009. *Petunia hybrida CAROTENOID CLEAVAGE DIOXYGENASE7* is involved in the production of negative and positive branching signals in *Petunia*. *Plant Physiology* **151**: 1867–1877.

Emanuelsson O, Nielsen H, von Heijne G. 1999. ChloroP, a neural network-based method for predicting chloroplast transit peptides and their cleavage sites. *Protein Science* **8**: 978–984.

Estrada AF, Maier D, Scherzinger D, Avalos J, Al-Babili S. 2008. Novel apocarotenoid intermediates in *Neurospora crassa* mutants imply a new biosynthetic reaction sequence leading to neurosporaxanthin formation. *Fungal Genetics and Biology* **45**: 1497–1505.

Foo E, Davies NW. 2011. Strigolactones promote nodulation in pea. *Planta* **234**: 1073–1081.

Frank W, Decker EL, Reski R. 2005. Molecular tools to study *Physcomitrella patens*. *Plant Biology* **7**: 220–227.

Fraser PD, Bramley PM. 2004. The biosynthesis and nutritional uses of carotenoids. *Progress in Lipid Research* **43**: 228–265.

Girke T, Schmidt H, Zahringer U, Reski R, Heinz E. 1998. Identification of a novel Delta 6-acyl-group desaturase by targeted gene disruption in *Physcomitrella patens*. *Plant Journal* **15**: 39–48.

Giuliano G, Al-Babili S, von Lintig J. 2003. Carotenoid oxygenases: cleave it or leave it. *Trends in Plant Science* **8**: 145–149.

Gomez-Roldan V, Fermas S, Brewer PB, Puech-Pagès V, Dun EA, Pillot J-P, Letisse F, Matusova R, Danoun S, Portais J-C *et al.* 2008. Strigolactone inhibition of shoot branching. *Nature* **455**: 189–194.

Gutjahr C, Parniske M. 2013. Cell and developmental biology of arbuscular mycorrhiza symbiosis. *Annual Review of Cell and Developmental Biology* **29**: 593–617.

Hamiaux C, Drummond RS, Janssen BJ, Ledger SE, Cooney JM, Newcomb RD, Snowden KC. 2012. DAD2 is an α/β hydrolase likely to be involved in the perception of the plant branching hormone, strigolactone. *Current Biology* **22**: 2032–2036.

Haugen JA, Englert G, Glinz E, Liaaen-Jensen S. 1992. Structural assignments of geometrical isomers of fucoxanthin. *Acta Chemica Scandinavica* **46**: 389–395.

Hoffmann B, Proust H, Belcram K, Labrune C, Boyer F-D, Rameau C, Bonhomme S. 2014. Strigolactones inhibit caulonema elongation and cell division in the moss *Physcomitrella patens*. *PLoS ONE* **9**: e99206.

Horst NA, Katz A, Pereman I, Decker EL, Ohad N, Reski R. 2016. A single homeobox gene triggers phase transition, embryogenesis and asexual reproduction. *Nature Plants* **2**: 15209.

Kapulnik Y, Koltai H. 2014. Strigolactone involvement in root development, response to abiotic stress, and interactions with the biotic soil environment. *Plant Physiology* **166**: 560–569.

Kapulnik Y, Koltai H. 2016. Fine-tuning by strigolactones of root response to low phosphate. *Journal of Integrative Plant Biology* **58**: 203–212.

Langdale JA. 2008. Evolution of developmental mechanisms in plants. *Current Opinion in Genetics & Development* **18**: 368–373.

Lavy M, Prigge MJ, Tao S, Shain S, Kuo A, Kirchsteiger K, Estelle M. 2016. Constitutive auxin response in *Physcomitrella* reveals complex interactions between Aux/IAA and ARF proteins. *eLife* **5**: e13325.

Lehtonen MT, Akita M, Kalkkinen N, Ahola E, Rönnholm G, Somervuo P, Thelander M, Valkonen JPT. 2009. Quickly released peroxidase of moss (*Physcomitrella patens*) in defense against fungal invaders. *New Phytologist* **183**: 432–443.

Lin H, Wang R, Qian Q, Yan M, Meng X, Fu Z, Yan C, Jiang B, Su Z, Li J *et al.* 2009. DWARF27, an iron-containing protein required for the biosynthesis of strigolactones, regulates rice tiller bud outgrowth. *Plant Cell* **21**: 1512–1525.

von Lintig J. 2012. Metabolism of carotenoids and retinoids related to vision. *Journal of Biological Chemistry* **287**: 1627–1634.

Lopez-Obando M, Conn CE, Hoffmann B, Bythell-Douglas R, Nelson DC, Rameau C, Bonhomme S. 2016. Structural modelling and transcriptional responses highlight a clade of PpKAI2-LIKE genes as candidate receptors for strigolactones in *Physcomitrella patens*. *Planta* **243**: 1441–1453.

Ludwig-Müller J, Jülke S, Bierfreund NM, Decker EL, Reski R. 2009. Moss (*Physcomitrella patens*) GH3 proteins act in auxin homeostasis. *New Phytologist* **181**: 323–338.

Medina HR, Cerdá-Olmedo E, Al-Babili S. 2011. Cleavage oxygenases for the biosynthesis of trisporoids and other apocarotenoids in *Phycomyces*. *Molecular Microbiology* **82**: 199–208.

Menand B, Yi K, Jouannic S, Hoffmann L, Ryan E, Linstead P, Schaefer DG, Dolan L. 2007. An ancient mechanism controls the development of cells with a rooting function in land plants. *Science* **316**: 1477–1480.

Moise AR, Al-Babili S, Wurtzel ET. 2014. Mechanistic aspects of carotenoid biosynthesis. *Chemical Reviews* **114**: 164–193.

Moise AR, von Lintig J, Palczewski K. 2005. Related enzymes solve evolutionarily recurrent problems in the metabolism of carotenoids. *Trends in Plant Science* **10**: 178–186.

Morris SE, Turnbull CG, Murfet IC, Beveridge CA. 2001. Mutational analysis of branching in pea. Evidence that *Rms1* and *Rms5* regulate the same novel signal. *Plant Physiology* **126**: 1205–1213.

Nelson D, Werck-Reichhart D. 2011. A P450-centric view of plant evolution. *Plant Journal* **66**: 194–211.

Nisar N, Li L, Lu S, Khin NC, Pogson BJ. 2015. Carotenoid metabolism in plants. *Molecular Plant* **8**: 68–82.

Paponov IA, Teale W, Lang D, Paponov M, Reski R, Rensing SA, Palme K. 2009. The evolution of nuclear auxin signalling. *BMC Evolutionary Biology* **9**: 126.

Prigge MJ, Bezanilla M. 2010. Evolutionary crossroads in developmental biology: *Physcomitrella patens*. *Development* **137**: 3535–3543.

Proust H, Hoffmann B, Xie X, Yoneyama K, Schaefer DG, Yoneyama K, Nogué F, Rameau C. 2011. Strigolactones regulate protonema branching and act as a quorum sensing-like signal in the moss *Physcomitrella patens*. *Development* **138**: 1531–1539.

Rensing SA, Lang D, Zimmer AD, Terry A, Salamov A, Shapiro H, Nishiyama T, Perroud P-F, Lindquist EA, Kamisugi Y *et al.* 2008. The *Physcomitrella* genome reveals evolutionary insights into the conquest of land by plants. *Science* **319**: 64–69.

Ruch S, Beyer P, Ernst HG, Al-Babili S. 2005. Retinal biosynthesis in eubacteria: *in vitro* characterization of a novel carotenoid oxygenase from *Synechocystis* sp. PCC 6803. *Molecular Microbiology* **55**: 1015–1024.

Ruyter-Spira C, Al-Babili S, van der Krol S, Bouwmeester H. 2013. The biology of strigolactones. *Trends in Plant Science* **18**: 72–83.

de Saint Germain A, Bonhomme S, Boyer F-D, Rameau C. 2013. Novel insights into strigolactone distribution and signalling. *Current Opinion in Plant Biology* **16**: 583–589.

Schwartz SH, Tan BC, Gage DA, Zeevaart JA, McCarty DR. 1997. Specific oxidative cleavage of carotenoids by VP14 of maize. *Science* **276**: 1872–1874.

Seto Y, Sado A, Asami K, Hanada A, Umehara M, Akiyama K, Yamaguchi S. 2014. Carlactone is an endogenous biosynthetic precursor for strigolactones. *Proceedings of the National Academy of Sciences, USA* **111**: 1640–1645.

Seto Y, Yamaguchi S. 2014. Strigolactone biosynthesis and perception. *Current Opinion in Plant Biology* **21**: 1–6.

Simons JL, Napoli CA, Janssen BJ, Plummer KM, Snowden KC. 2007. Analysis of the *DECREASED APICAL DOMINANCE* genes of *Petunia* in the control of axillary branching. *Plant Physiology* **143**: 697–706.

Sorefan K, Booker J, Haurogné K, Goussot M, Bainbridge K, Foo E, Chatfield S, Ward S, Beveridge C, Rameau C *et al.* 2003. *MAX4* and *RMS1* are orthologous dioxygenase-like genes that regulate shoot branching in *Arabidopsis* and pea. *Genes & Development* **17**: 1469–1474.

Stumpe M, Göbel C, Faltin B, Beike AK, Hause B, Himmelsbach K, Bode J, Kramell R, Wasternack C, Frank W *et al.* 2010. The moss *Physcomitrella patens* contains cyclopentenones but no jasmonates: mutations in allene oxide cyclase lead to reduced fertility and altered sporophyte morphology. *New Phytologist* **188**: 740–749.

Torres-Vera R, García JM, Pozo MJ, López-Ráez JA. 2014. Do strigolactones contribute to plant defence? *Molecular Plant Pathology* **15**: 211–216.

Trautmann D, Beyer P, Al-Babili S. 2013. The ORF slr0091 of *Synechocystis* sp. PCC6803 encodes a high-light induced aldehyde dehydrogenase converting apocarotenals and alkanals. *FEBS Journal* **280**: 3685–3696.

Ueno K, Furumoto T, Umeda S, Mizutani M, Takikawa H, Batchvarova R, Sugimoto Y. 2014. Heliolactone, a non-sesquiterpene lactone germination stimulant for root parasitic weeds from sunflower. *Phytochemistry* **108**: 122–128.

Umehara M, Hanada A, Yoshida S, Akiyama K, Arite T, Takeda-Kamiya N, Magome H, Kamiya Y, Shirasu K, Yoneyama K *et al.* 2008. Inhibition of shoot branching by new terpenoid plant hormones. *Nature* **455**: 195–200.

Vandenbussche F, Fierro AC, Wiedemann G, Reski R, Van Der Straeten D. 2007. Evolutionary conservation of plant gibberellin signalling pathway components. *BMC Plant Biology* **7**: 65.

Viaene T, Landberg K, Thelander M, Medvecka E, Pederson E, Feraru E, Cooper ED, Karimi M, Delwiche CF, Ljung K *et al.* 2014. Directional auxin transport mechanisms in early diverging land plants. *Current Biology* **24**: 2786–2791.

Waldie T, McCulloch H, Leyser O. 2014. Strigolactones and the control of plant development: lessons from shoot branching. *Plant Journal* **79**: 607–622.

Walter MH, Strack D. 2011. Carotenoids and their cleavage products: biosynthesis and functions. *Natural Product Reports* **28**: 663–692.

Weng J-K, Chapple C. 2010. The origin and evolution of lignin biosynthesis. *New Phytologist* **187**: 273–285.

Xie X, Yoneyama K, Yoneyama K. 2010. The strigolactone story. *Annual Review of Phytopathology* **48**: 93–117.

Yoneyama K, Arakawa R, Ishimoto K, Kim HI, Kisugi T, Xie X, Nomura T, Kanampiu F, Yokota T, Ezawa T *et al.* 2015. Difference in *Striga*-susceptibility is reflected in strigolactone secretion profile, but not in compatibility and host preference in arbuscular mycorrhizal symbiosis in two maize cultivars. *New Phytologist* **206**: 983–989.

Yoneyama K, Xie X, Kim HI, Kisugi T, Nomura T, Sekimoto H, Yokota T, Yoneyama K. 2012. How do nitrogen and phosphorus deficiencies affect strigolactone production and exudation? *Planta* **235**: 1197–1207.

Yoneyama K, Yoneyama K, Takeuchi Y, Sekimoto H. 2007. Phosphorus deficiency in red clover promotes exudation of orobanchol, the signal for mycorrhizal symbionts and germination stimulant for root parasites. *Planta* **225**: 1031–1038.

Zhang Y, van Dijk ADJ, Scaffidi A, Flematti GR, Hofmann M, Charnikhova T, Verstappen F, Hepworth J, van der Krol S, Leyser O *et al.* 2014. Rice cytochrome P450 MAX1 homologs catalyze distinct steps in strigolactone biosynthesis. *Nature Chemical Biology* **10**: 1028–1033.

Zimmer AD, Lang D, Buchta K, Rombauts S, Nishiyama T, Hasebe M, Van de Peer Y, Rensing SA, Reski R. 2013. Reannotation and extended community resources for the genome of the non-seed plant *Physcomitrella patens* provide insights into the evolution of plant gene structures and functions. *BMC Genomics* **14**: 498.

Zou J, Zhang S, Zhang W, Li G, Chen Z, Zhai W, Zhao X, Pan X, Xie Q, Zhu L. 2006. The rice *HIGH-TILLERING DWARF1* encoding an ortholog of *Arabidopsis* MAX3 is required for negative regulation of the outgrowth of axillary buds. *Plant Journal* **48**: 687–698.

Supporting Information

Additional Supporting Information may be found online in the Supporting Information tab for this article:

Fig. S1 Sequence alignment of CCD7 enzymes from pea, rice, *Arabidopsis* and *Physcomitrella*.

Fig. S2 SDS-PAGE analysis of the expression of Thioredoxin-PpCCD7 and -PpCCD8.

Fig. S3 HPLC analysis of PpCCD7 incubations with different β-carotene isomers.

Fig. S4 HPLC analysis of PpCCD7 incubations with all-*trans*-carotenoids.

Fig. S5 LC-MS analysis of PpCCD7 products from incubation with 9- and 9′-*cis*-cryptoxanthin.

Fig. S6 HPLC analysis of PpCCD8 incubations with all-*trans*-substrates.

Fig. S7 HPLC analysis of PpCCD8 incubations with all-*trans*-carotenoids.

Fig. S8 HPLC analysis of PpCCD8 incubations with *cis*-configured C_{40}-carotenoids.

Fig. S9 RT-PCR from putative *Δ CCD7* and *Δ CCD8* lines.

Fig. S10 Southern analysis of *Δ CCD7* and *Δ CCD8* lines.

Fig. S11 *Orobanche ramosa* seed germination in the vicinity of *Δ CCD7* lines grown on standard Knop medium and on phosphate-deficient medium.

Fig. S12 *Fusarium oxysporum* infection at 3, 5, 7 and 9 d post infection (dpi).

Fig. S13 *Irpex* sp. infection at 3, 5, 7 and 9 d post infection (dpi).

Fig. S14 Growth inhibition of *Sclerotinia sclerotiorum* by the synthetic strigolactone analogue GR24.

Table S1 Primers used in this study

Table S2 International Moss Stock Center accession numbers

Table S3 *Orobanche ramosa* seed germination on standard Knop and on phosphate-deficient medium

Methods S1 Screening of transgenic plants

Methods S2 Southern analysis of *Δ CCD7* and *Δ CCD8* lines

Methods S3 Growth of *Sclerotinia* on GR24-containing medium

Please note: Wiley Blackwell are not responsible for the content or functionality of any Supporting Information supplied by the authors. Any queries (other than missing material) should be directed to the *New Phytologist* Central Office.